



Supplement of

**Ammonia emissions and depositions over the contiguous United States
derived from IASI and CrIS using the directional derivative approach**

Zitong Li et al.

Correspondence to: Kang Sun (kangsun@buffalo.edu) and Kaiyu Guan (kaiyug@illinois.edu)

The copyright of individual parts of the supplement might differ from the article licence.

Supplementary materials

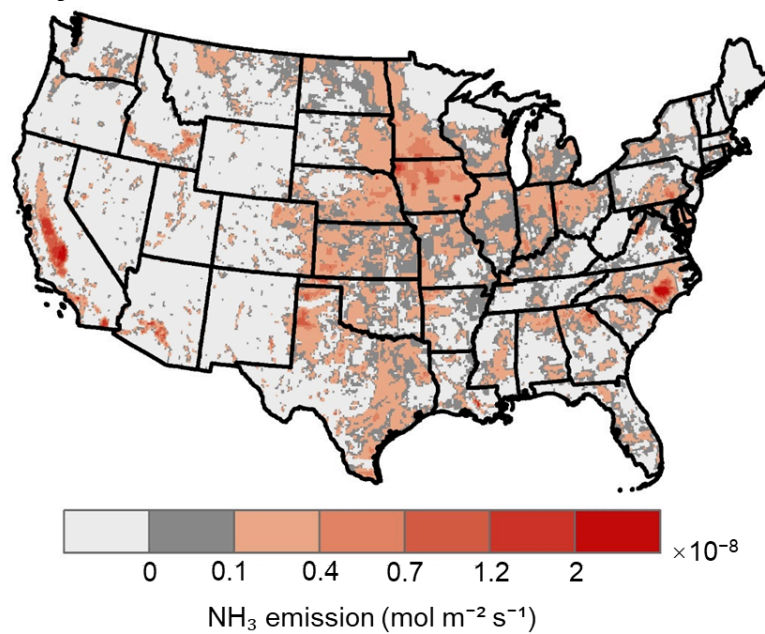
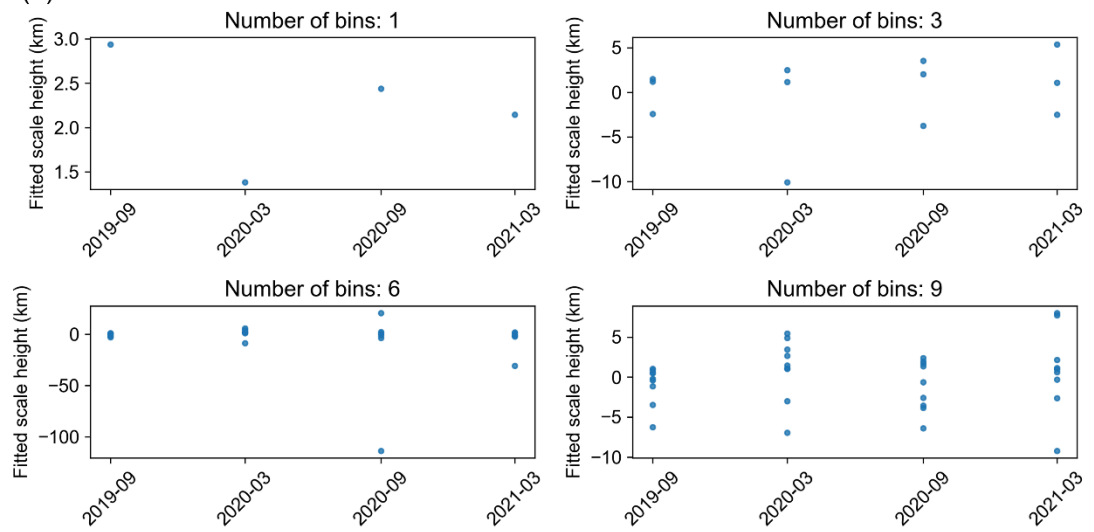


Figure S1. NH_3 emission from the Harmonized Emissions Component (HEMCO) version 3.0 for 2016 over the CONUS.

(a) IASI



(b) CrIS

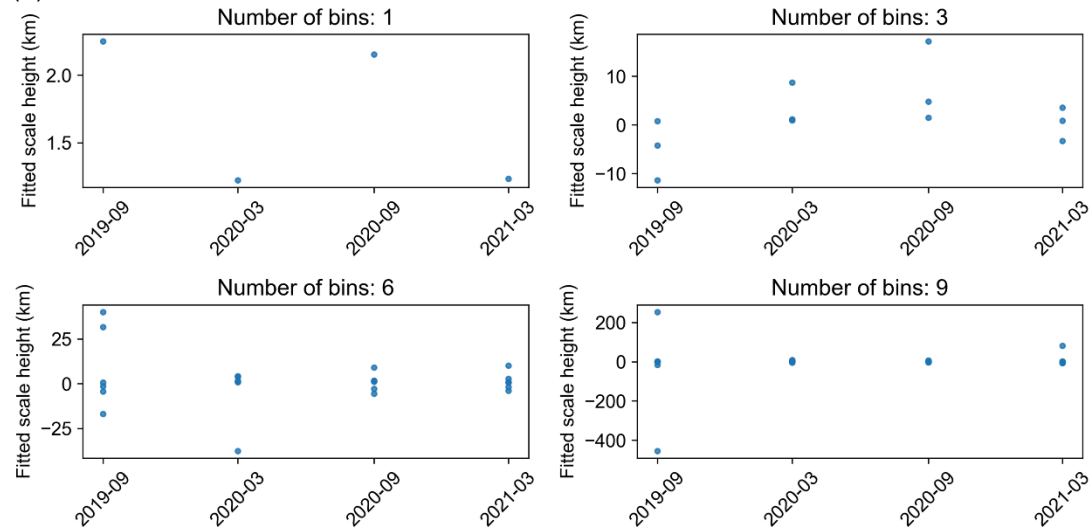


Figure S2. Spatial sensitivity tests for the topography term fitting to derive DD_topo from IASI (a) and CrIS (b). The number of bins indicates the wind-topography ($u_0 \cdot (\nabla z_0)$) sectors used in the fitting. The y-axis shows the fitted X .

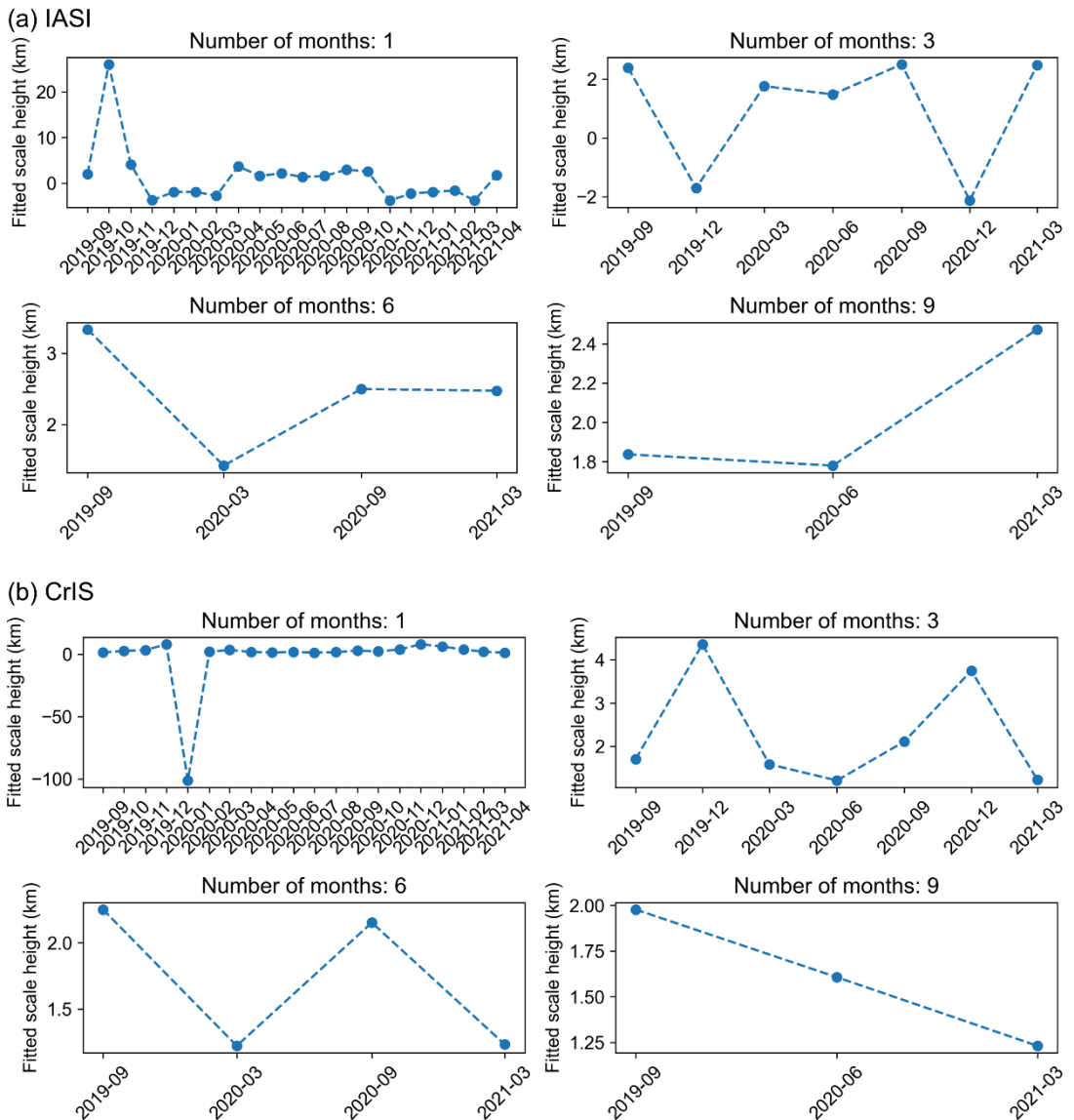


Figure S3. Temporal sensitivity tests for the topography term fitting to derive DD_topo from IASI (a) and CrIS (b). The number of months indicates the temporal aggregation interval used for the fitting. The y-axis shows the fitted X .

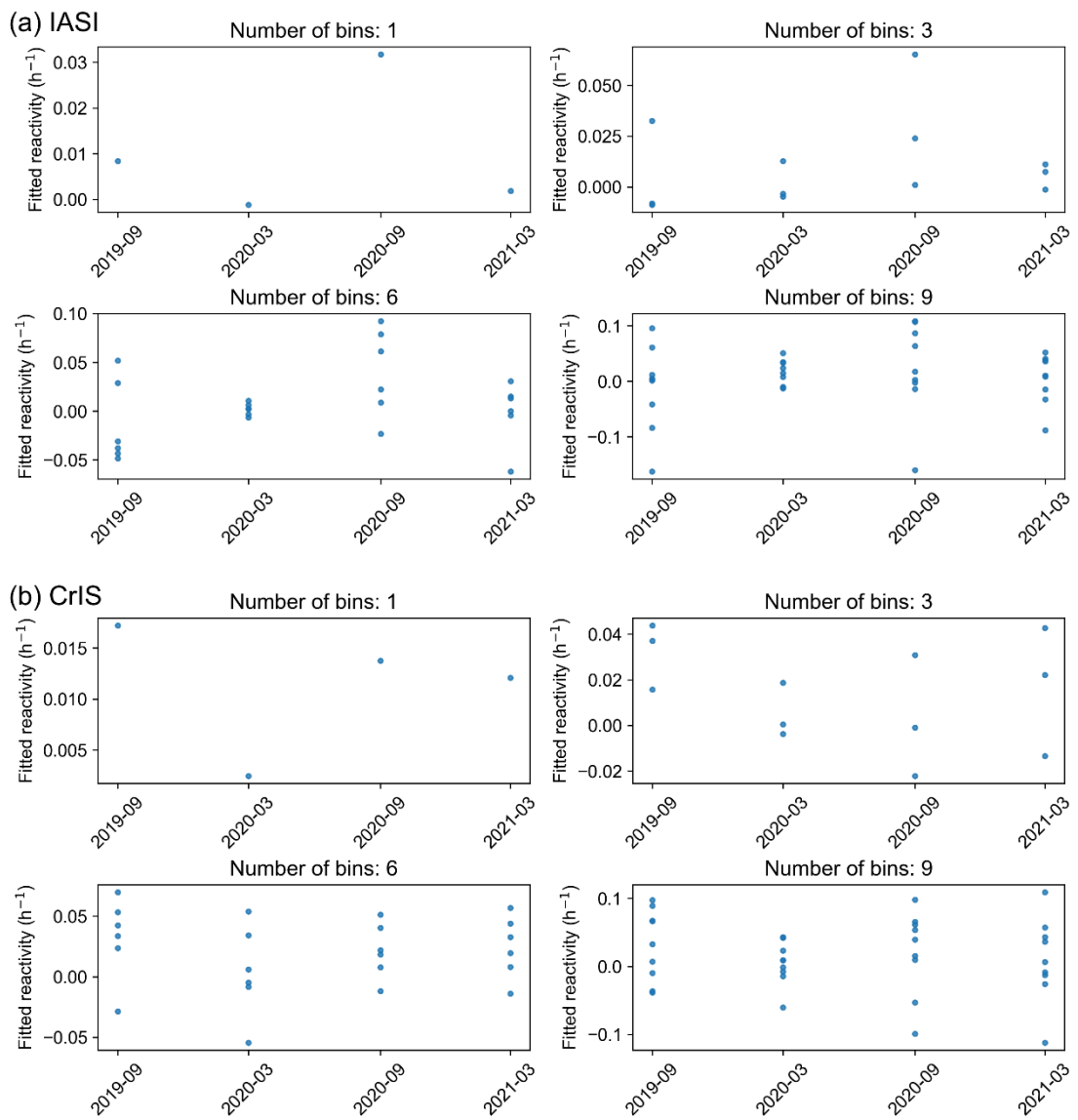


Figure S4. Spatial sensitivity tests for the chemistry term fitting to derive DD_chem from IASI (a) and CrIS (b). The number of bins indicates the column () sectors used in the fitting. The y-axis shows the fitted k .

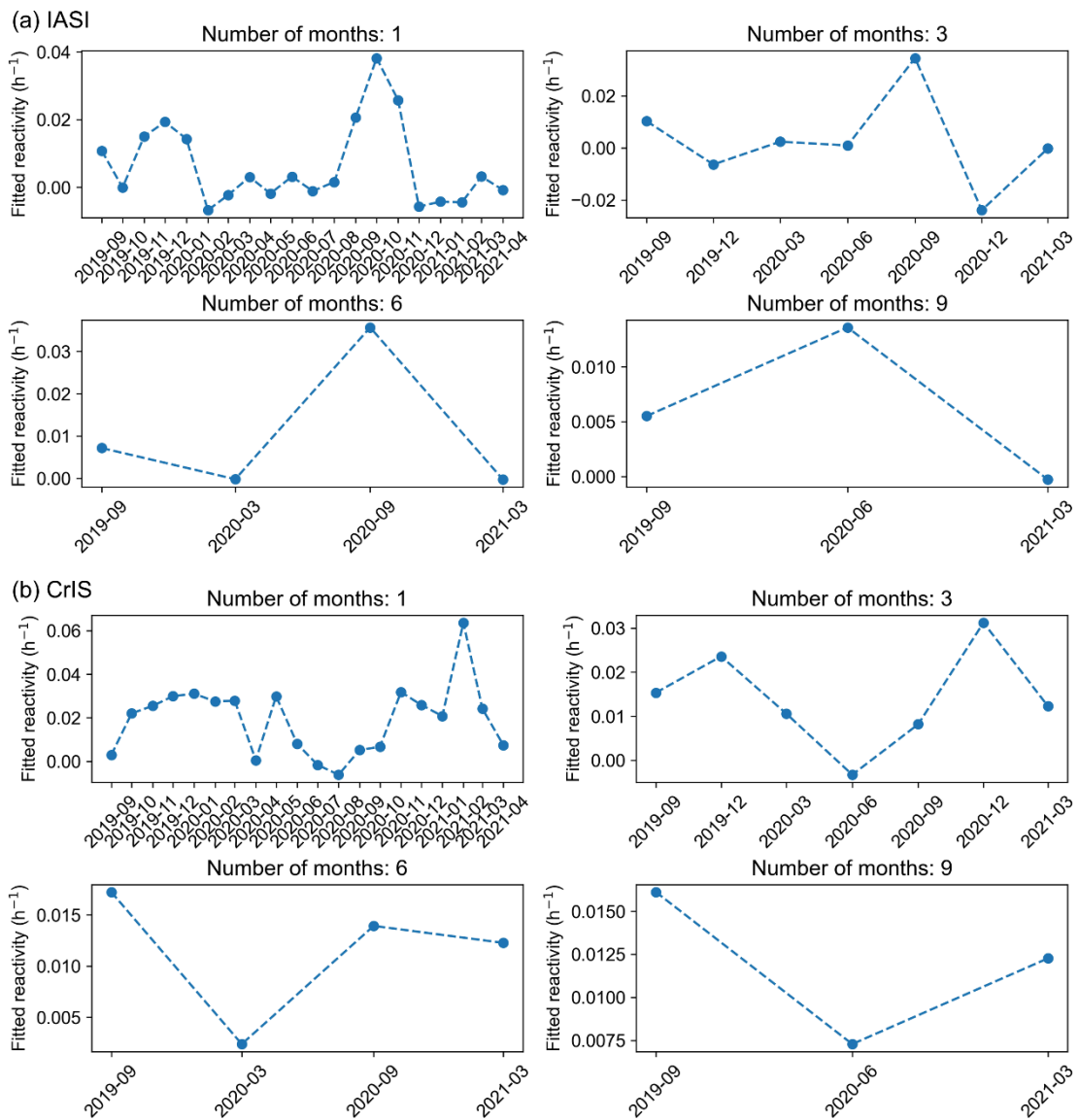


Figure S5. Temporal sensitivity tests for the chemistry term fitting to derive DD_{chem} from IASI (a) and CrIS (b). The number of months indicates the temporal aggregation interval used for the fitting. The y-axis shows the fitted k .

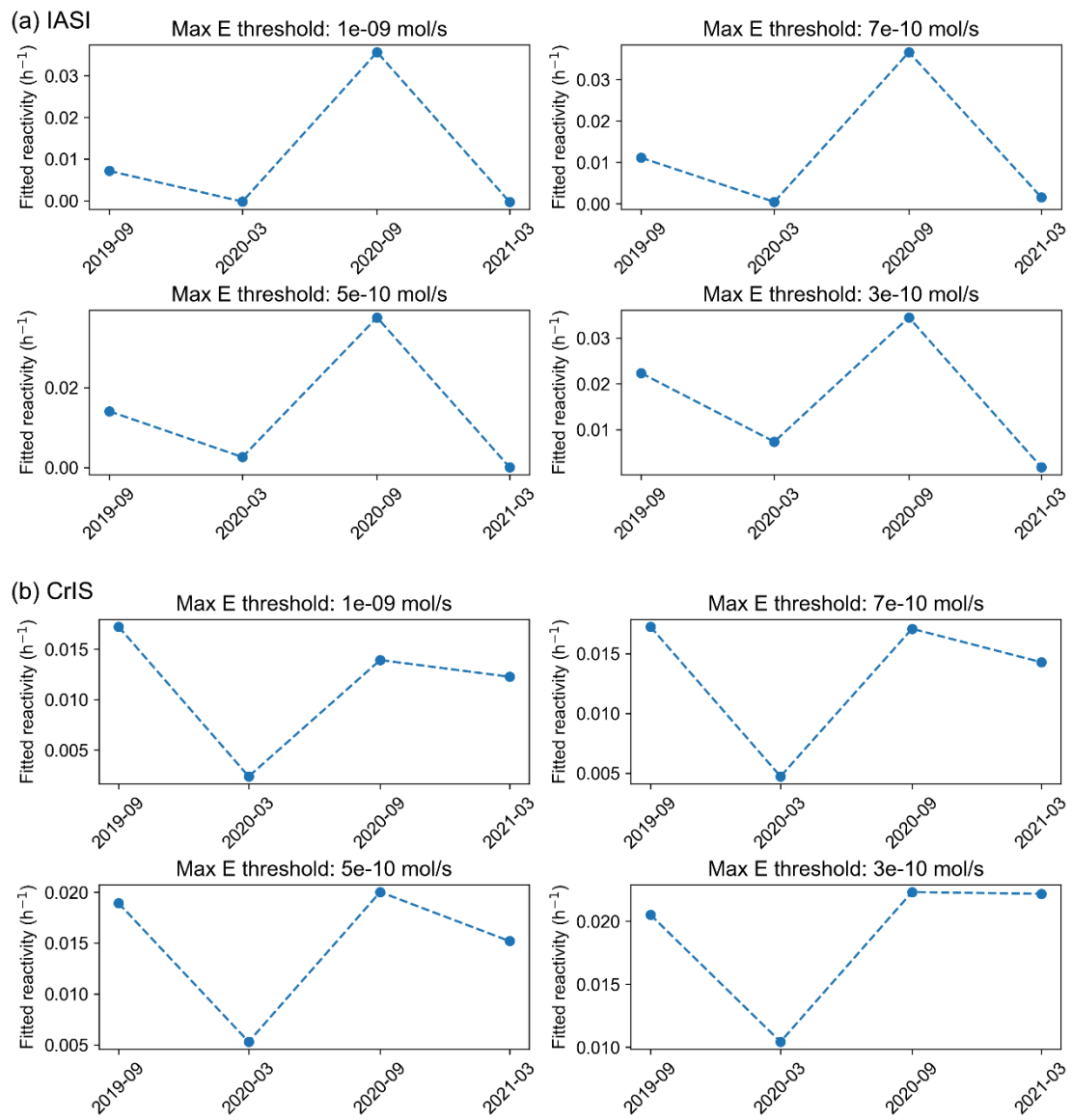


Figure S6. Maximum emission (E) threshold sensitivity tests for the chemistry term fitting to derive DD_chem from IASI (a) and CrIS (b). The y-axis shows the fitted k .

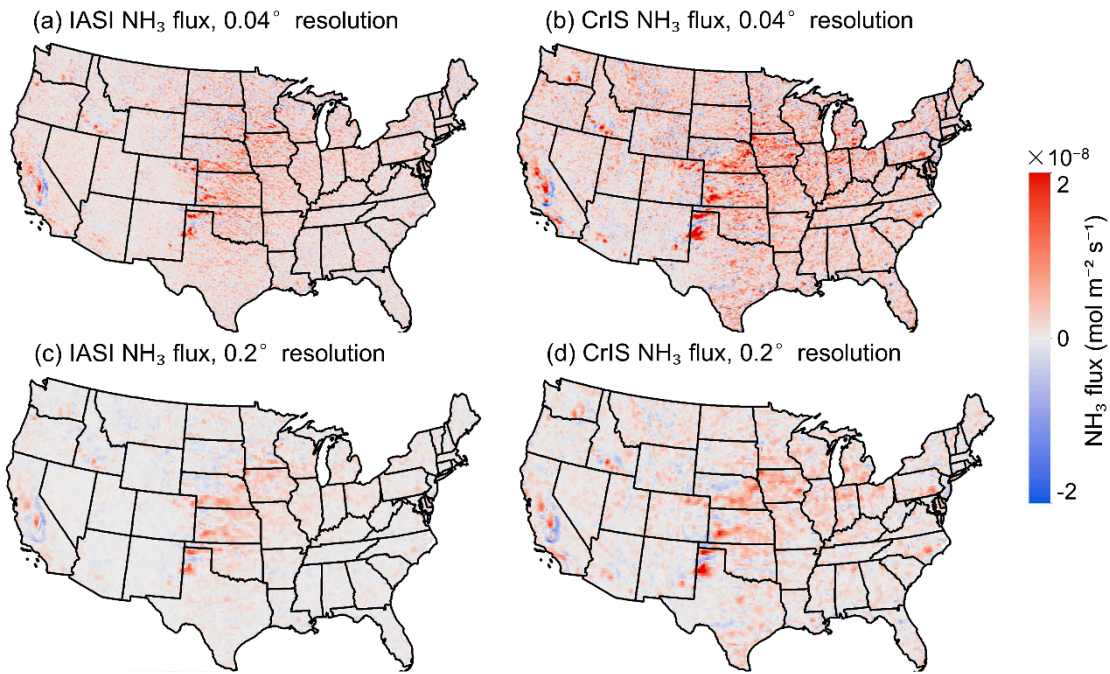


Figure S7. IASI- and CrIS-derived NH_3 fluxes (DD_chem estimator) averaged from Sep 2019 to Apr 2021 over the CONUS on a 0.04° and 0.2° grid.

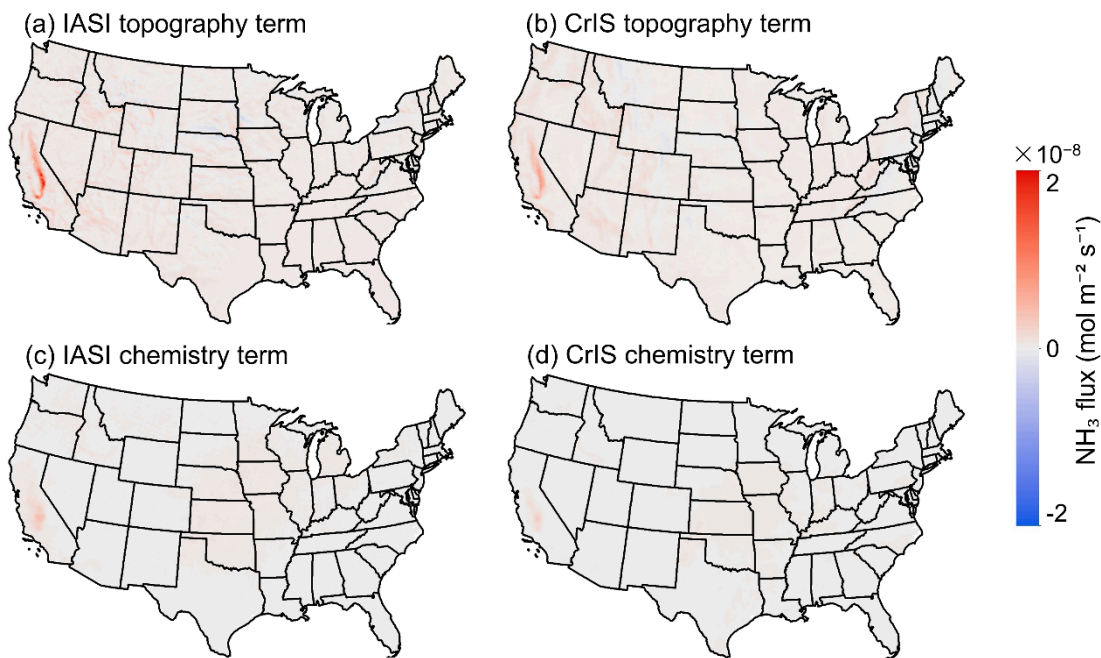


Figure S8. Topography and chemistry terms derived from IASI and CrIS from Sep 2019 to Apr 2021.

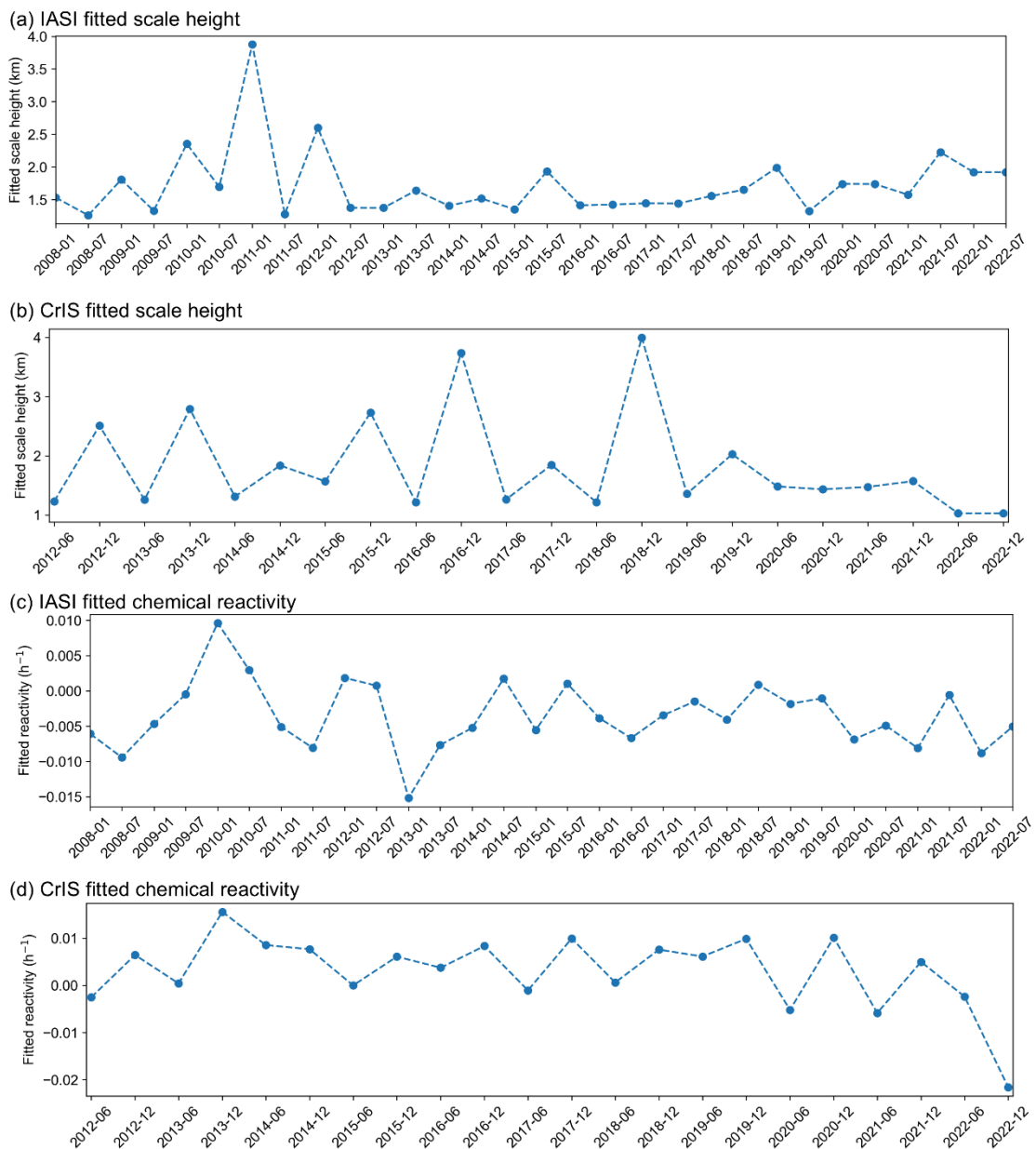


Figure S9. Fitted scale heights (a, b) and chemical reactivities (c, d) for IASI (a, c) and CrIS (b, d) records over the CONUS.

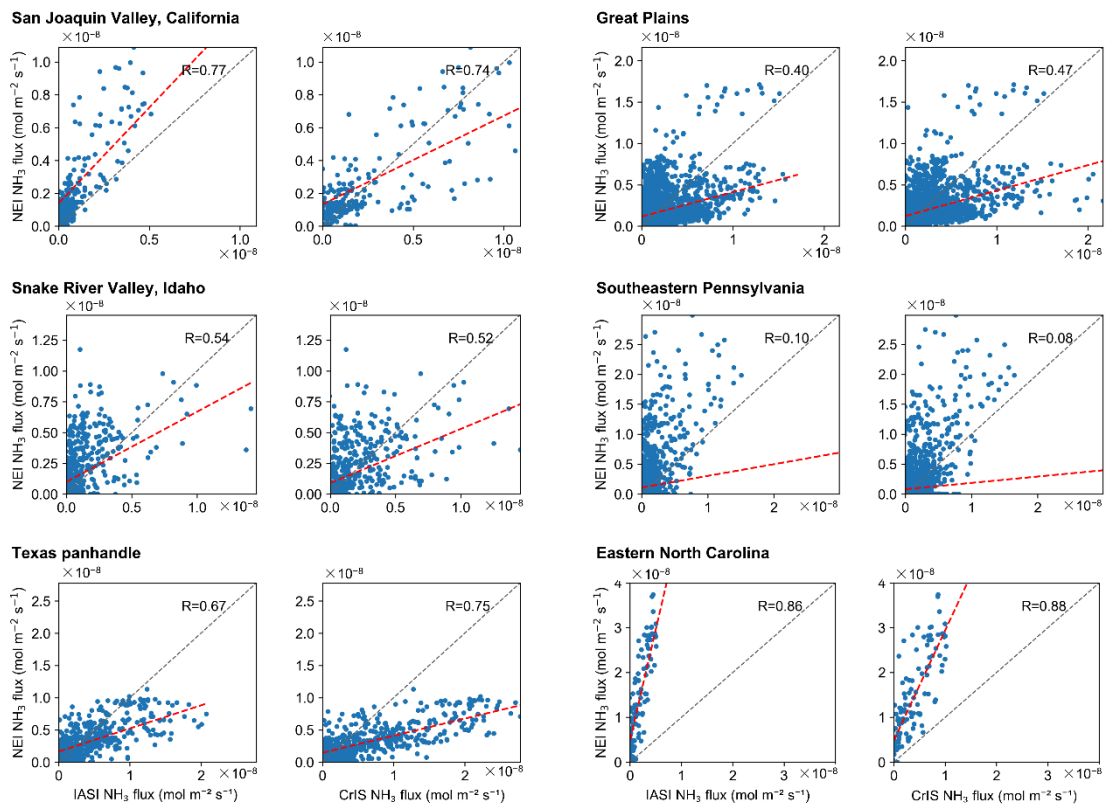


Figure S10. Satellite-based NH_3 fluxes from IASI and CrIS and inventory NH_3 fluxes in the San Joaquin Valley in California, Snake River Valley in Idaho, Texas panhandle, Great Plains, Southeastern Pennsylvania, and Eastern North Carolina.

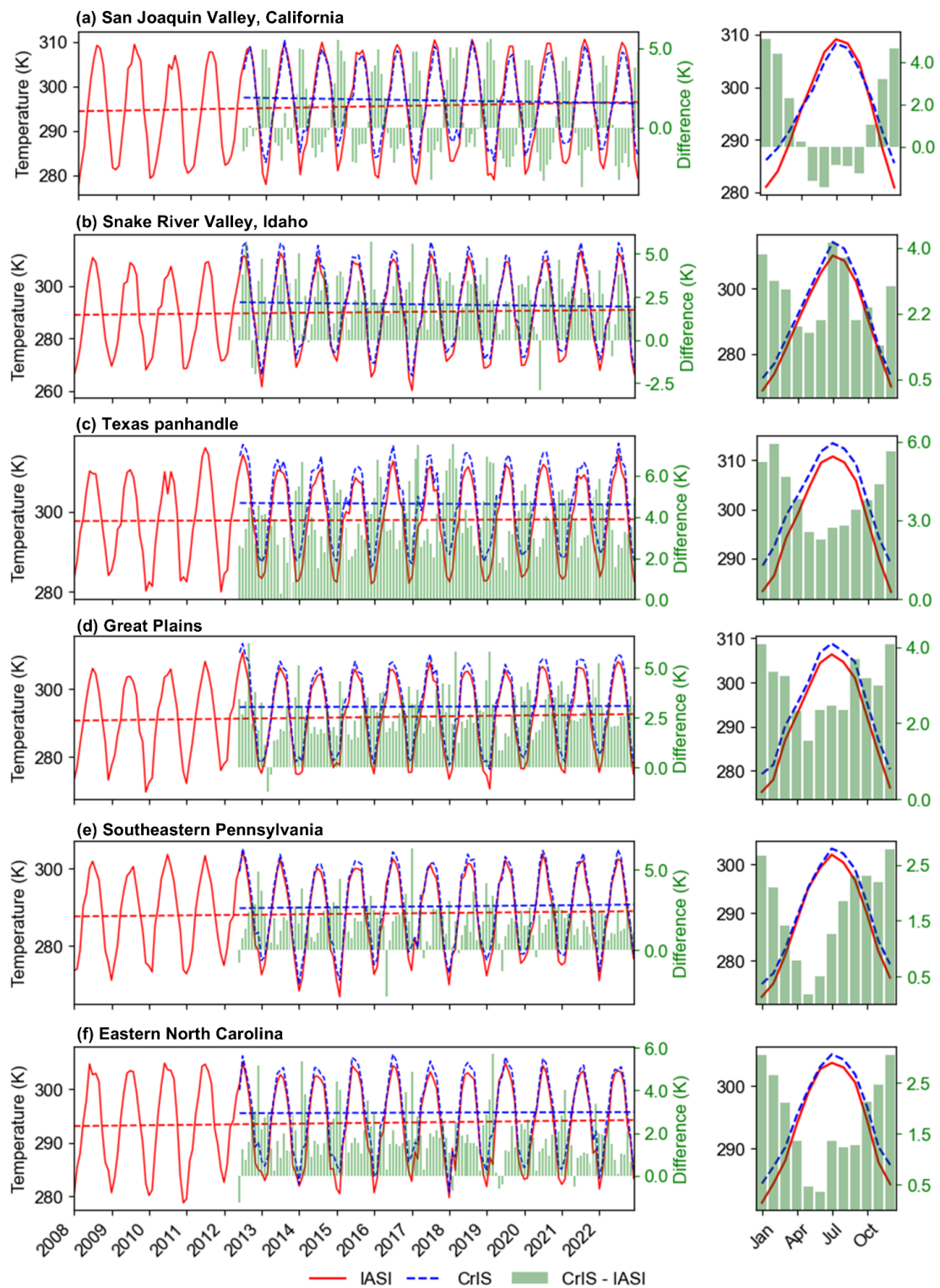


Figure S11. Surface temperature during the IASI (red solid lines) and CrIS (blue dashed lines) overpass in the San Joaquin Valley in California (a), Snake River Valley in Idaho (b), Texas panhandle (c), Great Plains (d), Southeastern Pennsylvania, and (f) Eastern North Carolina. Green bars represent the difference between CrIS and IASI.